Supporting information

Efficient Fully Textured Perovskite Silicon Tandems with Thermally Evaporated Hole Transporting Materials

Bhushan P. Kore[1,2], Oussama Er-raji[1,2], Oliver Fischer[1,2], Adrian Callies[1], Oliver Schultz-Wittmann[1], Patricia S. C. Schulze[1], Martin Bivour[1], Stefaan De Wolf[3], Stefan W. Glunz[1,2], Juliane Borchert[1,2]*

[1]Fraunhofer Institute for Solar Energy Systems ISE, Heidenhofstr. 2, 79110 Freiburg, Germany

[2]Chair of Photovoltaic Energy Conversion, Department of Sustainable Systems Engineering (INATECH), University of Freiburg, Emmy-Noether-Strasse 2, 79110 Freiburg, Germany

[3]Division of Physical Science and Engineering (PSE), King Abdullah University of Science and Technology (KAUST), Thuwal 23955-6900, Kingdom of Saudi Arabia

*Email: bhushan.kore@ise.fraunhofer.de

Experimental section

Silicon bottom cell fabrication: Silicon solar cells, used as a bottom solar cells in tandem devices, were fabricated using 250 µm thick p-doped silicon wafers (float zone) from Siltronic with 1 ohm cm base resistivity. Potassium hydroxide (KOH) was used for etching the Si wafer and get pyramidal texture on both side of the wafer. The pyramid size of 1 to 2 µm was achieved by controlling the rate and time of the reaction. In next step RCA cleaning was applied to clean the Si surface. A stack of intrinsic/doped amorphous silicon passivation layers was subsequently deposited on both sides of the wafer by using plasma-enhanced chemical vapor deposition (PECVD) in Indeotec cluster tool. The parallel-plate PECVD reactor was operated at 13,560 kHz and 200°C, utilizing a gas mixture of hydrogen (H2), trimethylboron (TMB), silane (SiH4), and phosphine (PH3). The thickness of the p-doped and n-doped layers was set to 12 nm, while the intrinsic layers were maintained at 6 nm, as shown in Figure 3a. A HF dipping treatment (aqueous solution of 1% hydrogen fluoride HF) was carried out to get rid of the SiO_2 from the surface. A structured recombination ITO layer (In_2O_3/SnO_2 = 90/10 wt% and using a mixture of oxygen and argon) with 1 cm^2 area was DC sputtered in Oxford instruments cluster tool. Likewise, on the back side a 195 nm thick ITO layer was DC sputtered but on full area of the wafer. To establish the back contact a 1000 nm thick silver layer was thermally evaporated. At last, the 4-inch wafer was laser separated in to 2.5 cm^2 area substrates with 1.1 cm^2 recombination ITO layer to build 1 cm^2 active area tandem devices. For large area tandem devices, a structured recombination ITO layer 2.1 x 2.1 cm was DC sputtered to build 7 tandem devices on one 4-inch wafer each with 4 cm^2 area, as shown in Figure 5c.

Perovskite top-cell fabrication: All the perovskite cells, including both single junction and tandems, were fabricated in the p-i-n configuration on textured Si substrate and textured Si bottom solar cells (BSCs). For a cell fabrication a cleaning procedure, consisting of dynamically spin-coating a 200 µL volume of ethanol at 2500 rpm for 30 s, was employed to remove unwanted dust particles on top of the surface. The textured Si bottom solar cells/ ohmic Si substrates were further cleaned with UV/ozone treatment for 15 min to get rid of the organic impurities from the surface. Different HTLs were deposited either by spin coating method or by thermal evaporation. 2PACz (referred as 2PACz SC or Ref. in the article, unless otherwise mentioned) was deposited with static spin coating technique. For this a 100 µL volume of a 7 mmol 2PACz (from Dyenamo) solution in ethanol was spin coated at 3000 rpm for 30 s with 7 s waiting time between dropping the solution on to the substrate till start of the spin-coating process followed by subsequent annealing at 100°C for 10 min. The thermal treatment ensured the conformal binding between the phosphonic group of the self-assembling molecules and the recombination ITO layer. Solution of 2PACz in ethanol was ultrasonicated before spin coating for 15 min to ensure the dissociation agglomerated particles in the solution.

2PACz (Dyenamo), TaTm (Dyenamo, 99.9%), Spiro-TTB (Lumtec, 99%) and Me-4PACz (Dyenamo) were thermally evaporated. The evaporation rate and temperature for different HTLs are as follows,

2PACz (0.15 Å/s at ~145 °C), TaTm (0.1 Å/s at ~320 °C), Spiro-TTB (0.2 Å/s at ~250 °C) and Me-4PACz (0.15 Å/s at ~145 °C). The thickness of the respective HTLs was monitored via quartz crystal balances and further measured using ellipsometry and SEM measurements. Note that for the evaporation of 2PACz each time a fresh material of 2PACz was used whereas for evaporation of other HTLs same materials was evaporated multiple times and were used without further annealing treatment.

For the perovskite layer formation, we used evaporation/spin-coating route or the so-called hybrid route. As a first step of the hybrid route an inorganic scaffold ~550 nm thick consisting of PbI_2 (beads from Alfa Aesar) and CsI (powder from Sigma-Aldrich) was thermally co-evaporated from ceramic crucibles sources using Lesker mini Spectros system. The thickness, evaporation rate and temperature for PbI_2 and CsI are as follows, PbI_2 (500 nm, 1 Å/s at ~280 °C) and CsI (50 nm, 0.1 Å/s at ~400 °C). The evaporation started at a base pressure of $< 2\times10^{-6}$ Torr, the substrate temperature was set to 20 °C during the evaporation and thickness of both the materials was monitored using quartz crystal balances.

For the second step, spin-coting of organo-halide salt solution a 0.67M solutions of FABr and FAI (Dyenamo) were prepared in ethanol (Dyenamo) and mixed together in 65/35 vol% of FABr/FAI after several hours of continuous stirring. For improving the perovskite crystallization, 3 mg/mL of urea an additive was also mixed in the solution of FABr/FAI. For spin-coating of organo-halide salts 150 µL of the FABr/FAI+Urea solution was dynamically spin coated on the inorganic scaffold with 2200 rpm for 35 s followed by an annealing in air at 100 °C for 10 mins. The perovskite crystallization takes place in ambient atmosphere with relative humidity varying from 25 to 60%.

After perovskite layer formation, a 21 nm thick electron transporting layer (ETL), C_{60} (TCI), was thermally evaporated at ~0.15 Å/s rate and ~ 470°C temperature with base pressure of $< 4\times10^{-6}$ Torr.

In the next step, 20 nm of SnOx buffer layer was deposited with atomic layer deposition technique at 80°C using de-ionized water (kept at room temperature) and tetrakis(dimethylamino)tin(IV) (TDMASn, kept at 50°C) precursors to prevent the damage to the ETL/Perovskite interface. The doses and purge times for TDMASn/ purge/ H_2O/ purge were 0.3 s/ 1 s/ 0.2 s/ 10 s, respectively.

After SnOx buffer layer, a 20 nm thick ITO layer was DC sputtered only on the active area of the cell with the help of a shadow mask. Finally, a 200 nm (800 nm for champion devices with different metallization design) thick Ag layer was thermally evaporated at 5 Å/s rate and the thickness was monitored via quartz crystal balance. Ag layer was evaporated using a shadow mask to define the 1 cm² active area with L shaped Ag fingers having widths of ~100 µm (line shaped fingers having widths of ~25 µm for champion devices).

To further boost the j_{SC} of the tandem devices an antireflective coating of 100 nm thick MgFx was thermally evaporated at 2 Å/s rate and thickness of the layer monitored via quartz crystal balance. No shadow mask was used for MgFx evaporation.

Characterization techniques

XRD: A Bruker D8 Advance diffractometer, equipped with a Cu anode at 40 mA/40 kV was used to perform X-ray diffraction (XRD) measurements. The step size was set at 0.3° and the time per step 0.1s.

SEM: Cross-sectional and top-view electron microscopy images were captured using a Zeiss with a Schottky emission SEM (model Auriga 60, In lens detector). The acceleration voltage was set to 5 kV.

AFM: Atomic force microscopy (AFM) measurements were performed in PeakForce Tapping® mode using a Dimension Edge AFM (Bruker) with SCANASYST-AIR probes (Bruker). AFM images were recorded on area of 2×2 μm, using a resolution of 1024 ×1024 pixels.

Spectrally resolved PL: Steady-state photoluminescence (PL) measurements were performed using a LUQY Pro from Quantum Yield Berlin. A 532 nm laser was used as source of excitation with laser spot size of 0.1 cm^2 and 3 s resolution time. The equivalent laser intensity was varied from 0.05 sun to 1.2 sun for intensity-dependent iV_{OC} measurements.

UV-Vis: Reflectance and transmittance measurements were performed on a lambda 950 spectrometer (PerkinElmer) tool, in the wavelength range of 300-1200 nm were collected.

Contact angle measurements: Contact angle measurements were carried out using the 'contact angle system oca' setup from dataphysics. Water was used as a liquid for contact angle measurements. 5 uL of water droplets were dispensed on the planar substrates and the contact angle was fitted using the software SCA20. The final value was calculated as the mean of the left and right contact angles of the drop on the surface of different HTLs. The contact angles reported here are average of contact angle made by 4 droplets on the surface of different HTLs.

***jV* measurements:** *jV* measurements were performed suing a Wacom solar simulator equipped with two filtered lamps, a halogen and xenon lamp. The spectral response of a representative cell from each variation was measured before the *jV* measurements. Then the lamp intensities were calculated according to the method described by Meusel *et al*.[1] and adjusted using two filtered WPVS reference solar cells. A Keithley 2400 source meter was used to record *jV* curves in both forward and reverse directions over a voltage range of -100 to 1900 mV, with a scan speed of 34 mV/s and in 20 mV steps. The solar cell was maintained in open-circuit condition between the measurement points. All measurements were conducted in air on a temperature-controlled chuck set at 25°C.

***EQE*:** The external quantum efficiency was measured as described in our previous publication.[2] Note that the measured *EQE*s are not absolute.[3]

PESA: The Photoemission Spectroscopy in Air (PESA) measurements are carried out on the Riken AC-2 setup.

Suns-V_{OC}: A system developed at Fraunhofer ISE and constructed by Intego GmbH was used for the measurement of Suns-V_{OC}. For sub-cell selective excitation, the lasers with distinct wavelengths of 450 and 808 nm were used. A source meter, Höcherl & Hackl GmbH, NL20V20C24, was electrically connected to the cell in order to measure the V_{OC}. Finally, Pseudo-jV curves were constructed by varying the intensity of the illumination and measuring the V_{OC}.

Suns-PLI: The same setup that was used for Suns-V_{OC} measurements was also used to measure Suns-PL images. For sub-cell selective excitation, the lasers with distinct wavelengths of 450 and 808 nm were used. The cells were kept under constant illumination (under open-circuit conditions) to reach their stabilized state prior to taking an image of the perovskite sub-cells. Further details about the method can be found in Fischer et al.[4]

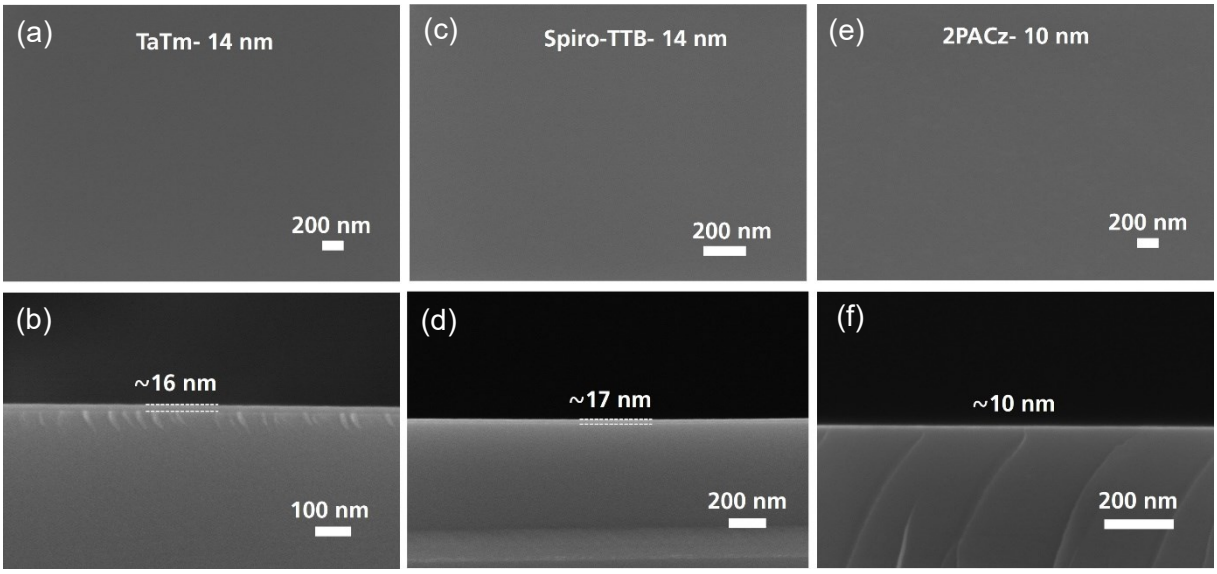

Figure S1. Top view and cross sectional view SEM images of thermally evaporated (a, b) 14 nm thick TaTm layer, (c,d) 14 nm thick Spiro-TTB layer and (e,f) 10 nm thick 2PACz layer. In case of 2PACz the layer was not quite visible. There is an error of 5 nm in the estimation of the thickness therefore for the better estimation of the thickness of HTL layer ellipsometry measurements were performed.

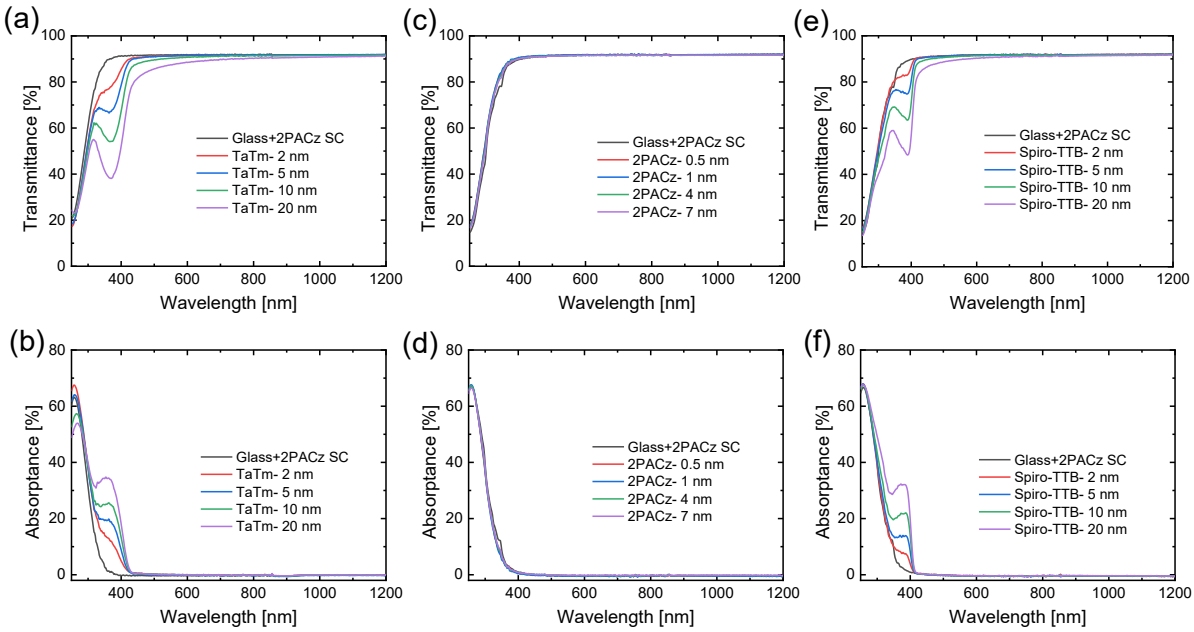

Figure S2. Transmittance and absorptance spectra of thermally evaporated (a,b) TaTm, (c,d) 2PACz and (e,f) Spiro-TTB with Glass/HTL stack. For comparison the transmittance and absorptance spectra of spin coated 2PACz (labelled 2PACz SC) is also plotted.

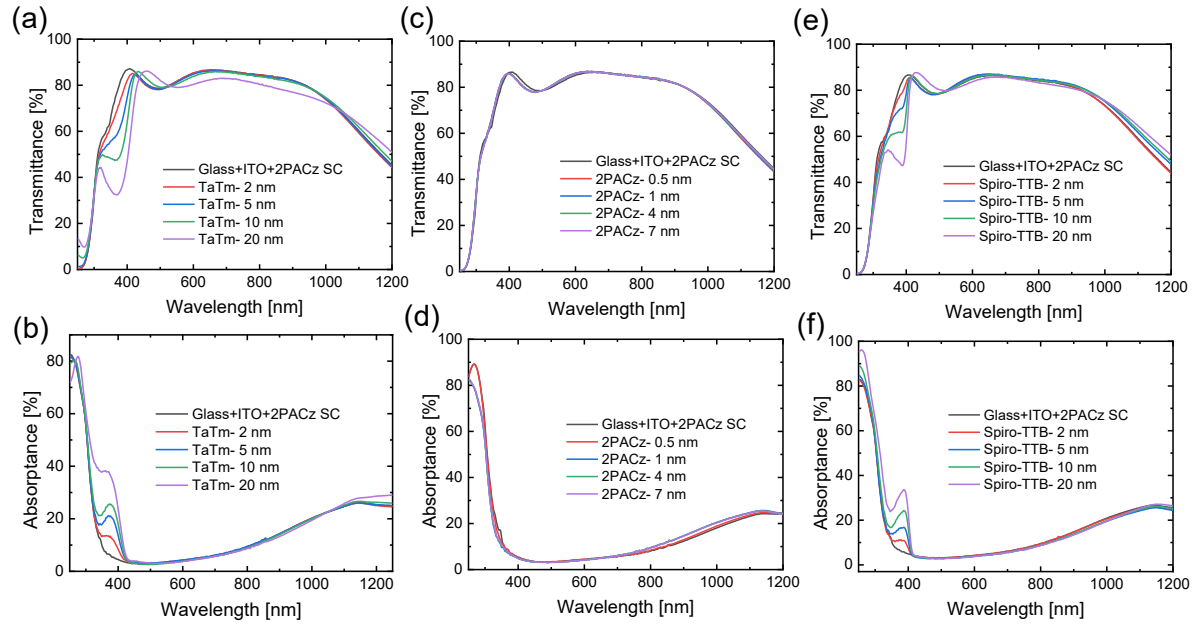

Figure S3. Transmittance and absorptance spectra of thermally evaporated (a,b) TaTm, (c,d) 2PACz and (e,f) Spiro-TTB with Glass/ITO/HTL stack. For comparison the transmittance and absorptance spectra of spin coated 2PACz (labelled 2PACz SC) is also plotted.

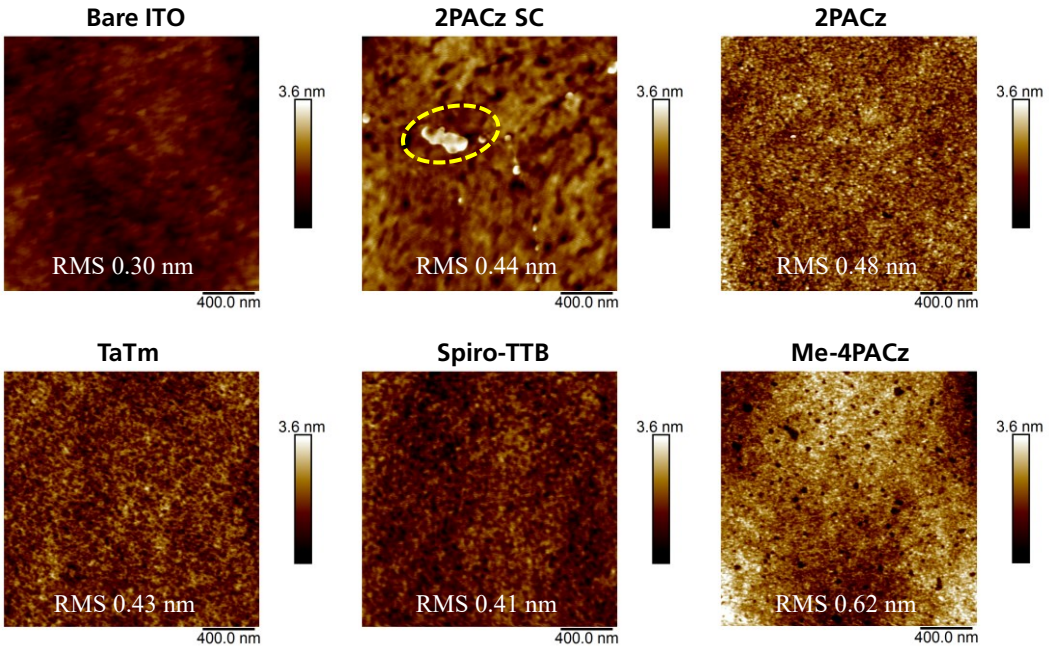

Figure S4. Atomic force microscopy (AFM) measurements of planar silicon/ITO/HTL stacks of bare ITO, spin coated 2PACz (7 mmol), evaporated 2PACz (4 nm), evaporated TaTm (5 nm), evaporated Spiro-TTB (10 nm) and evaporated Me-4PACz (4 nm).

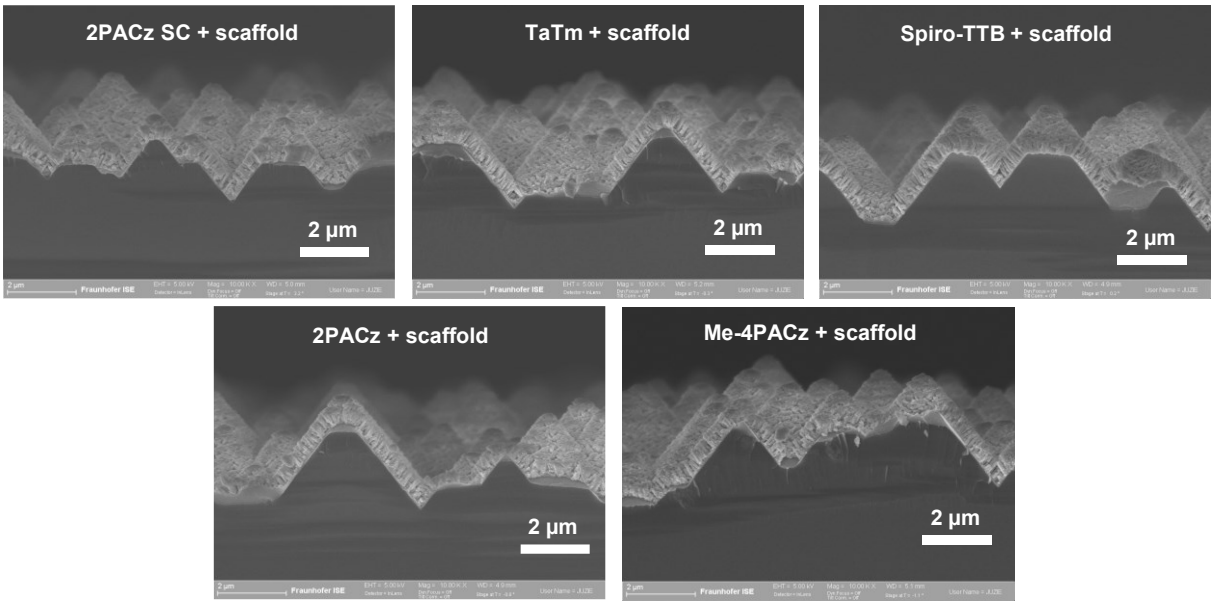

Figure S5. Cross sectional SEM images of thermally evaporated PbI_2:CsI scaffold (~550 nm thick) on different HTLs with textured silicon/ITO/HTL/scaffold stack.

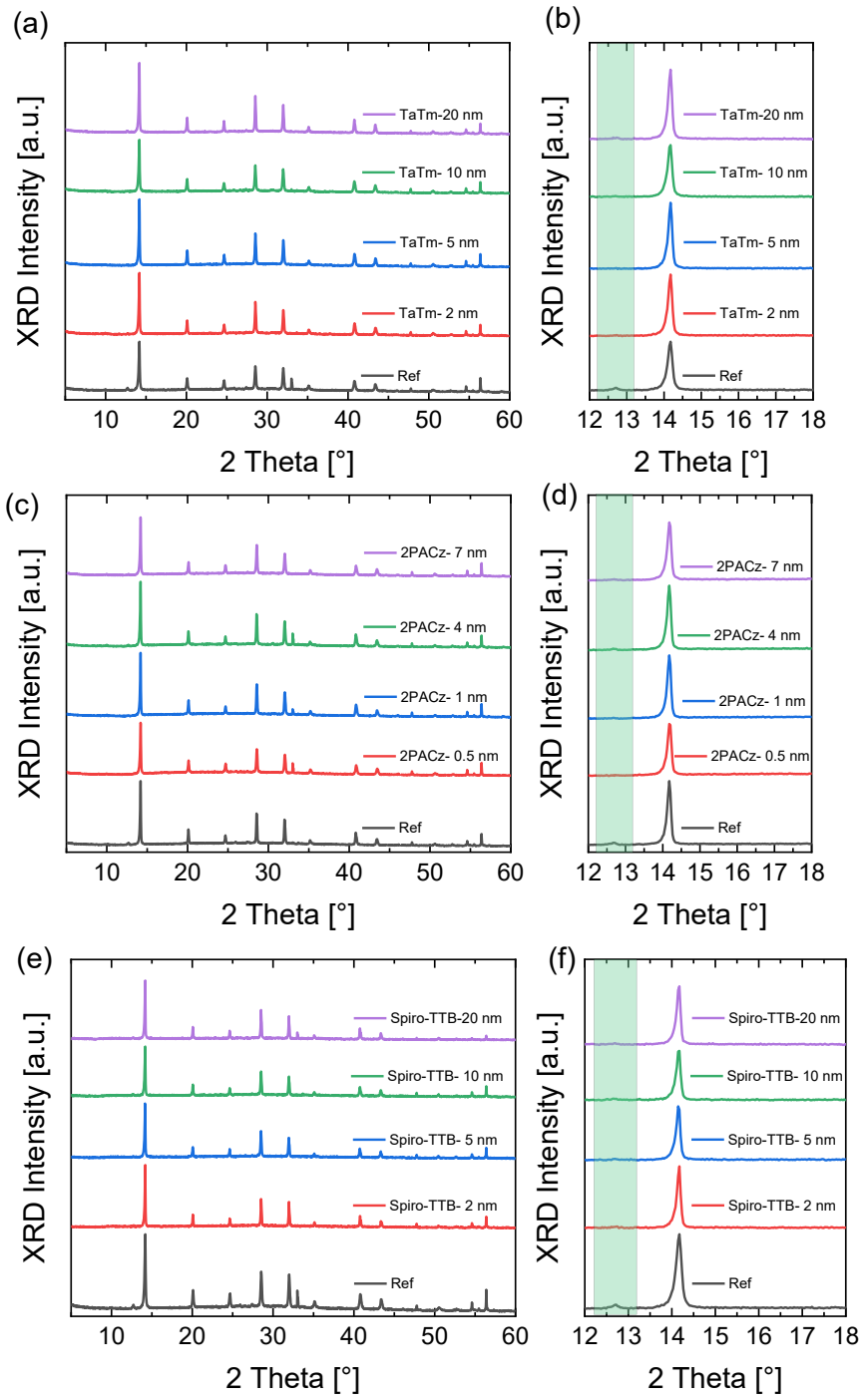

Figure S6. XRD patterns of perovskite processed on textured silicon/ITO/HTL/perovskite substrates with different HTLs (a,b) TaTm, (c,d) 2PACz and (e,f) Spiro-TTB and varying thickness of HTLs.

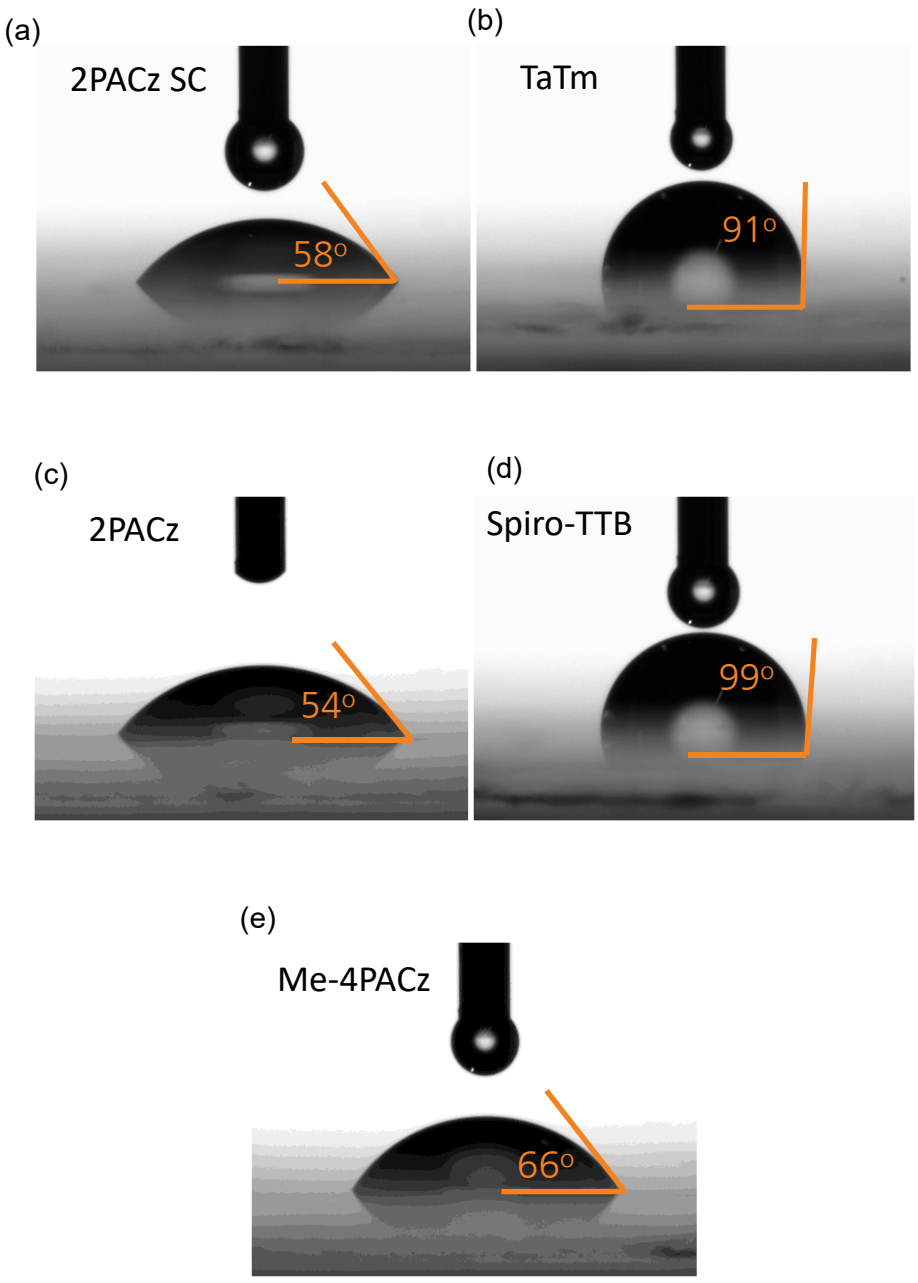

Figure S7. Contact angle measurement on glass/ITO/HTL stack for (a) spin-coated 2PACz, (b) TaTm, (c) 2PACz, (d) Spiro-TTB and (e) Me-4PACz.

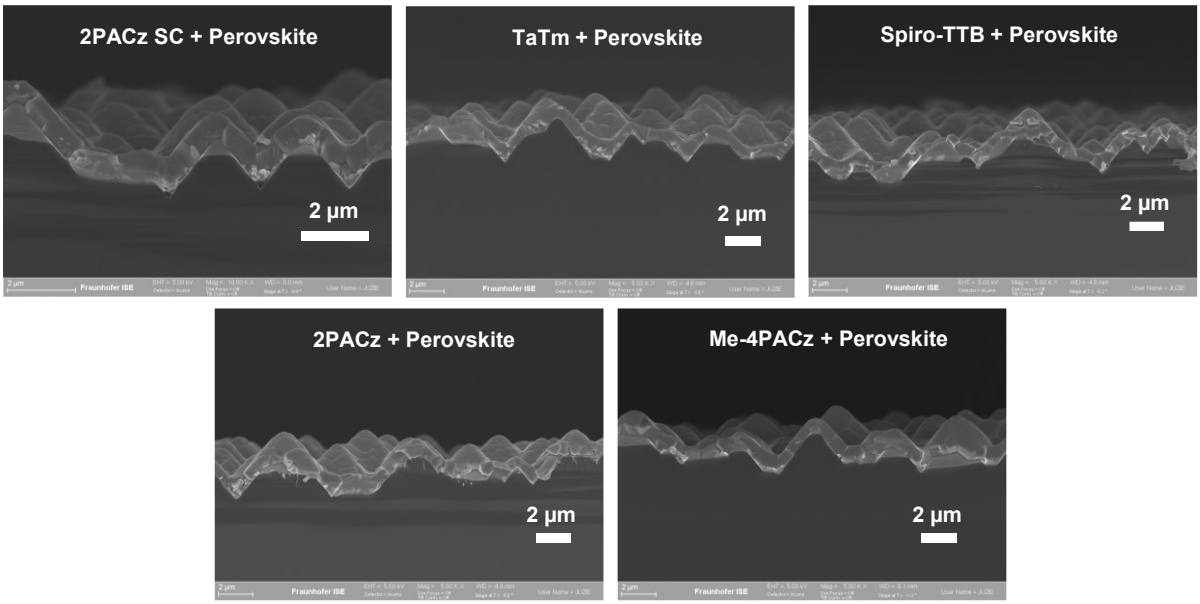

Figure S8. Cross sectional SEM images of perovskite on different HTLs with textured silicon/ITO/HTL/perovskite stack.

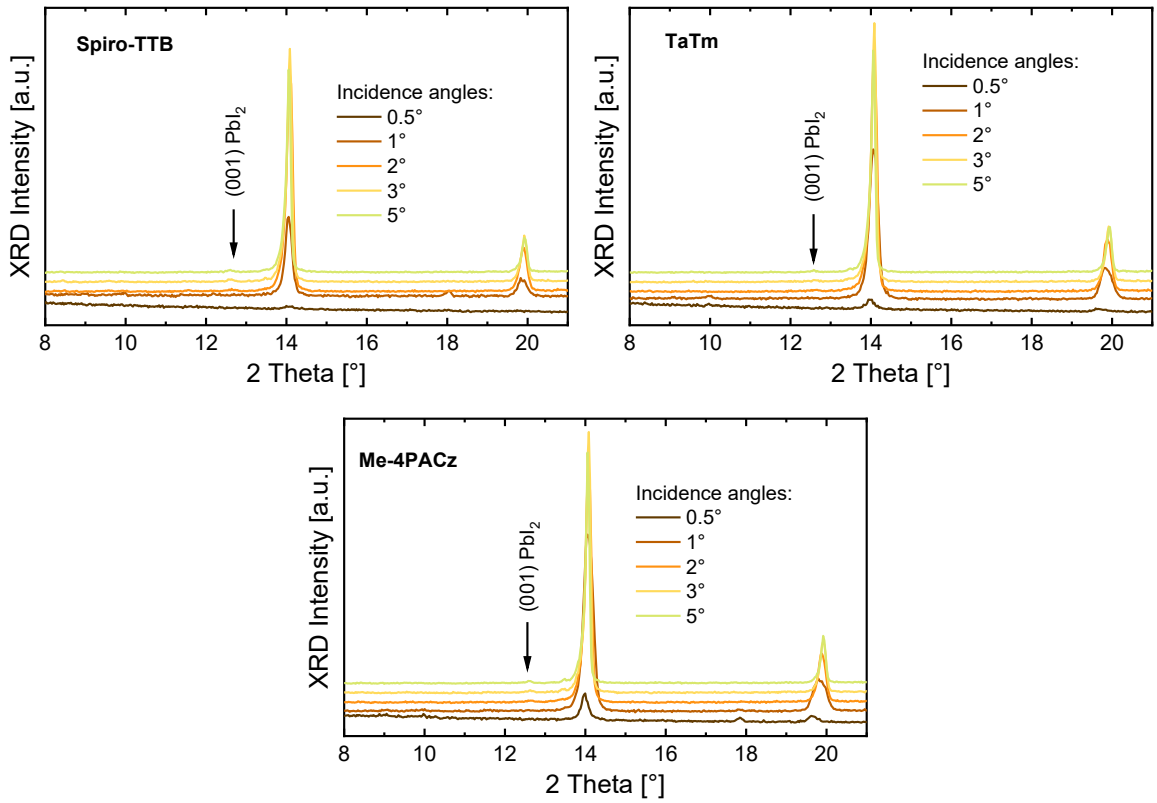

Figure S9. Grazing-incidence XRD diffractograms of perovskite films with different incident beam angles. The perovskite processed on Spiro-TTB, TaTm and Me-4PACz with textured silicon/ITO/HTL/perovskite configuration.

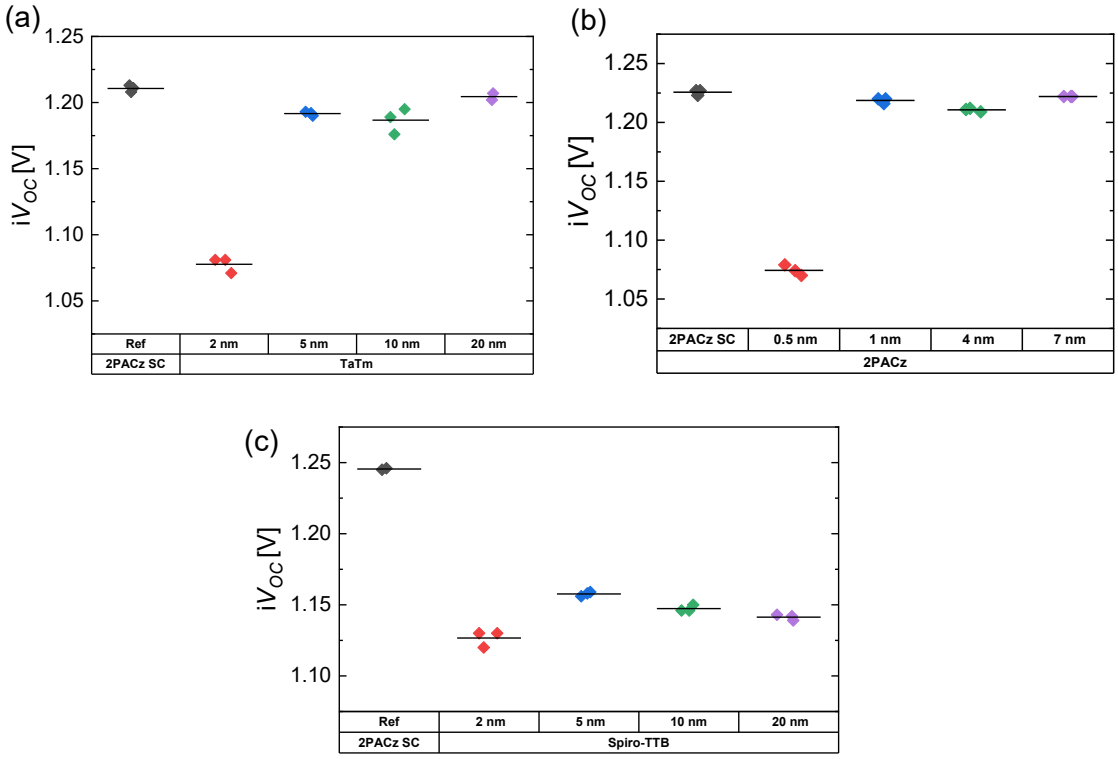

Figure S10: Comparison of the implied iV_{OC} for textured silicon/ITO/HTL/perovskite stack with thermally evaporated (a) TaTm, (b) 2PACz and (c) Spiro-TTB in comparison with spin coated 2PACz.

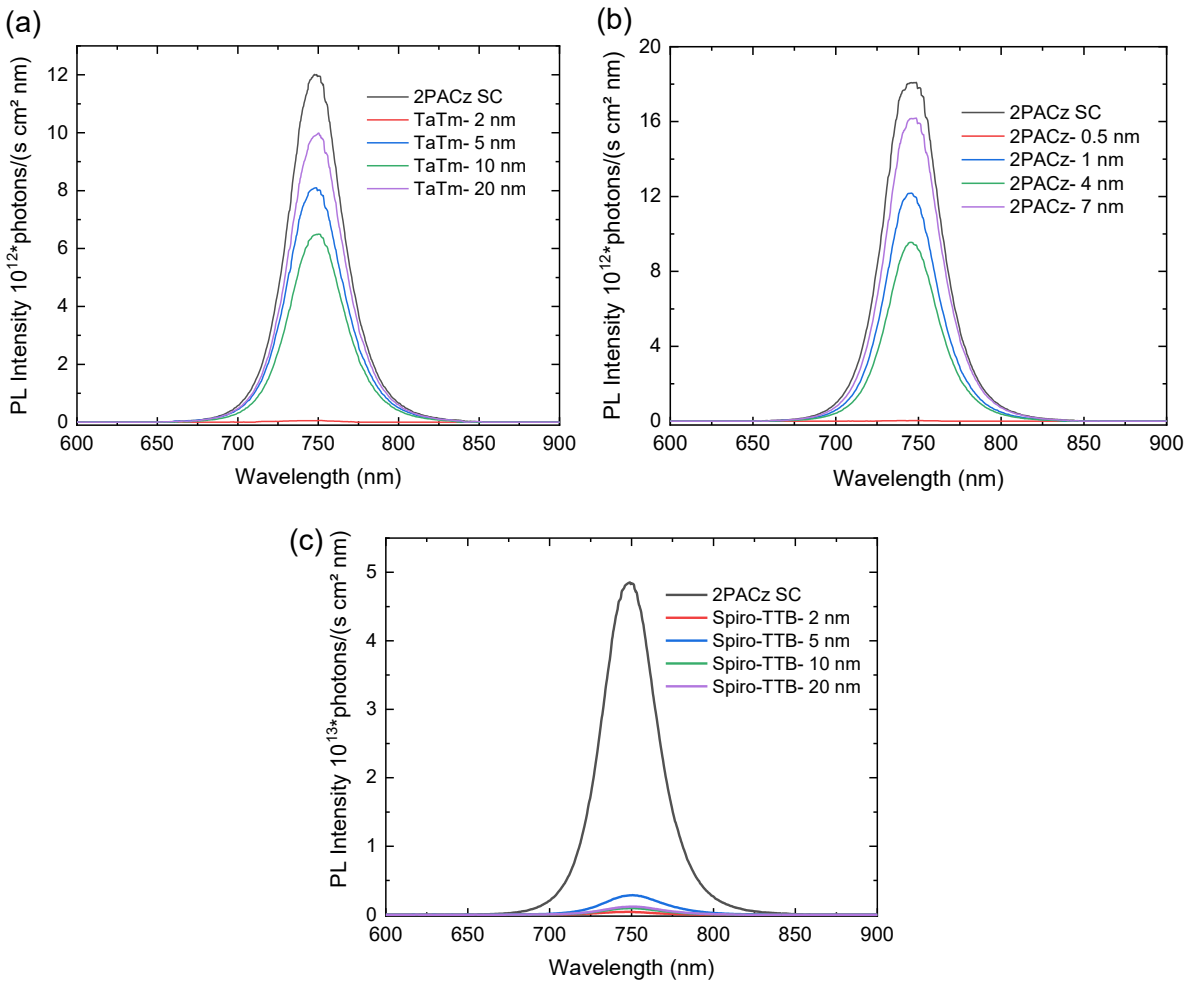

Figure S11. Comparison of steady state photoluminescence (PL) of perovskite layer processed on different HTLs with variation in thickness of (a) TaTm, (b) 2PACz and (c) Spiro-TTB.

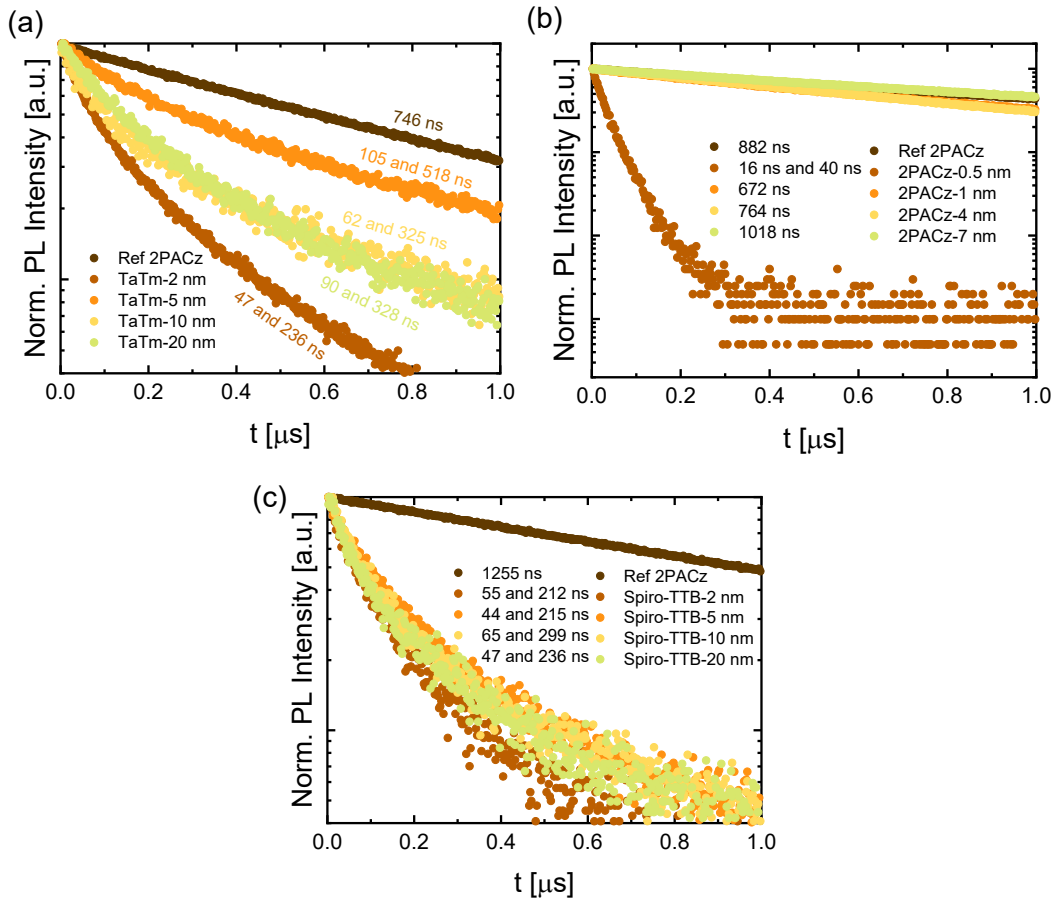

Figure S12. Transient PL decay curves of perovskite processed on different HTLs with varying thickness. The decay curves were exponentially fitted using single exponential and bi-exponential decay functions. The shorter lifetime component is attributed to presence of lossy HTL/perovskite interface whereas the longer lifetime component represents radiative recombination within perovskite.

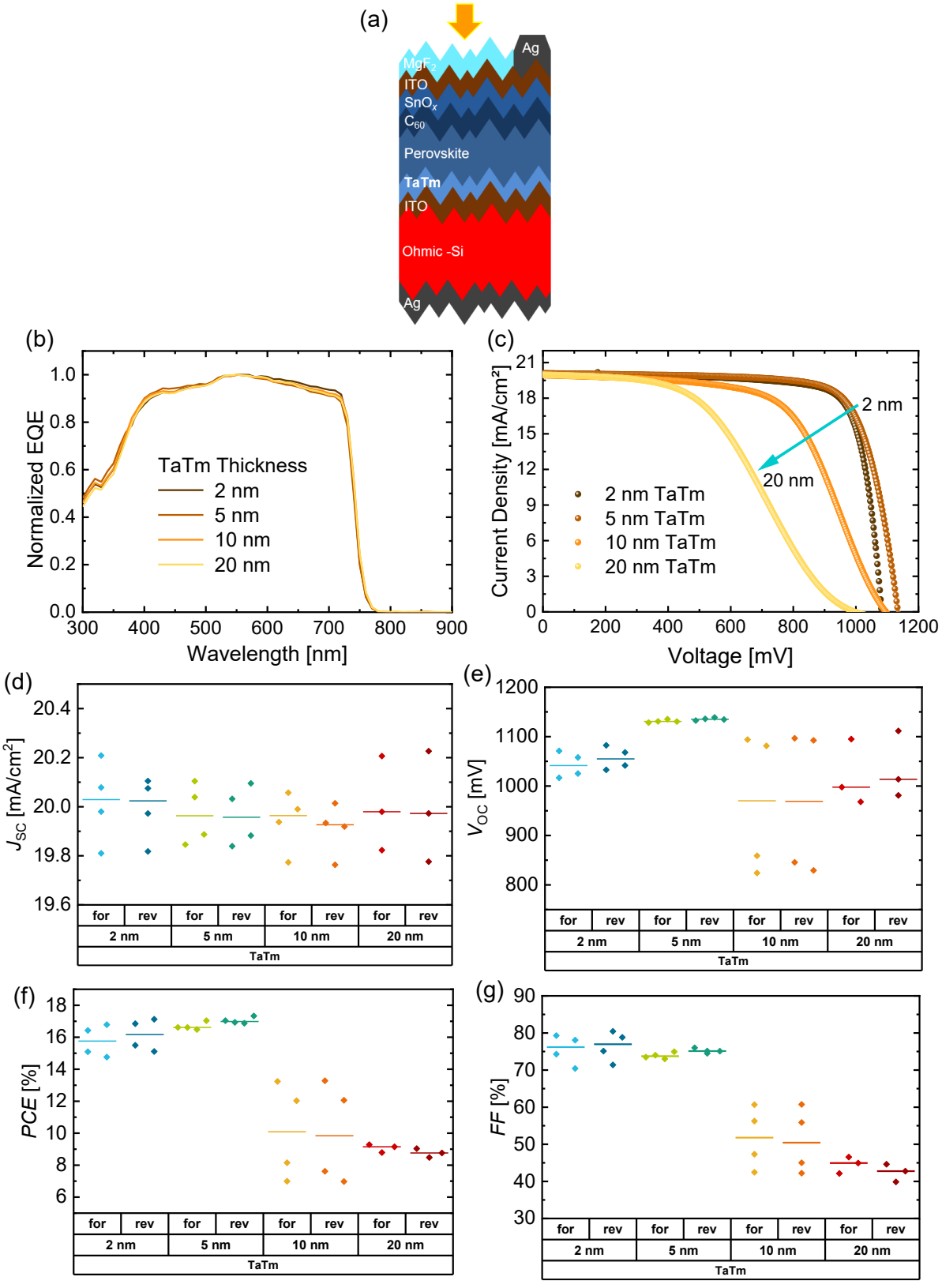

Figure S13. (a) Solar cell configuration of single junction perovskite cell processed on textured ohmic silicon substrate. (b) Normalized *EQE* of single junction solar cells for different thickness of TaTm. (c) *jV* curves of the best performing cells from each group scanned in reverse direction (V_{OC} to j_{SC}). (d, e, f, g) Influence of varying the thickness of the TaTm layer on the *jV* parameters of single junction solar cells fabricated in p-i-n configuration.

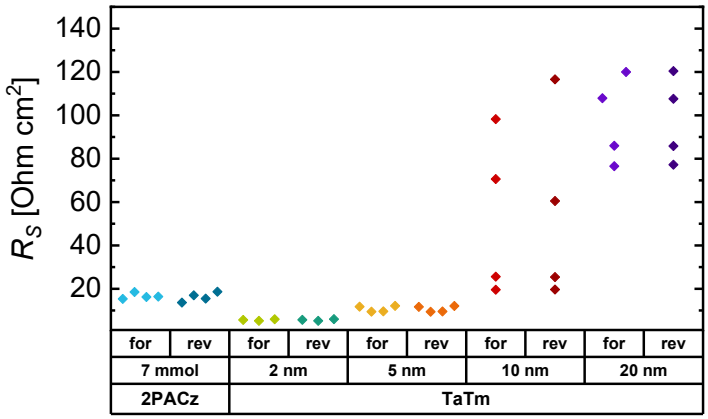

Figure S14. Variation in the effective series resistance (R_s) of the tandem devices with increase in the thickness of the TaTm layer, calcultaed from the slope of the jV curves near the V_{OC} of tandem devices.

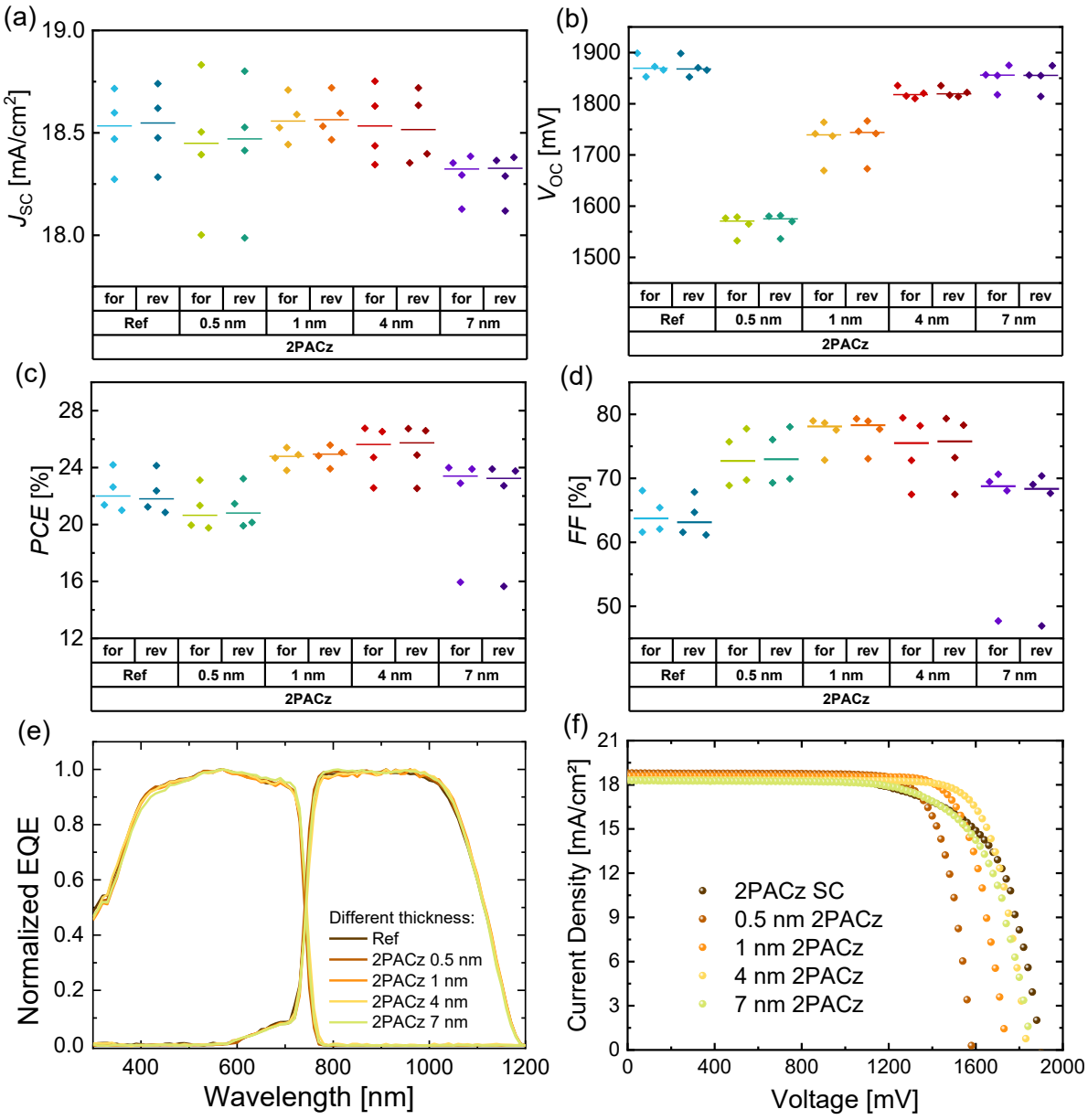

Figure S15. (a, b, c, d) Influence of varying the thickness of the 2PACz layer on the *jV* parameters of perovskite silicon tandems solar cells fabricated in p-i-n configuration. (e) Normalized *EQE* of tandem solar cells for different thickness of 2PACz. (f) *jV* curves of the best performing cells from each group scanned in reverse direction (V_{OC} to j_{SC}).

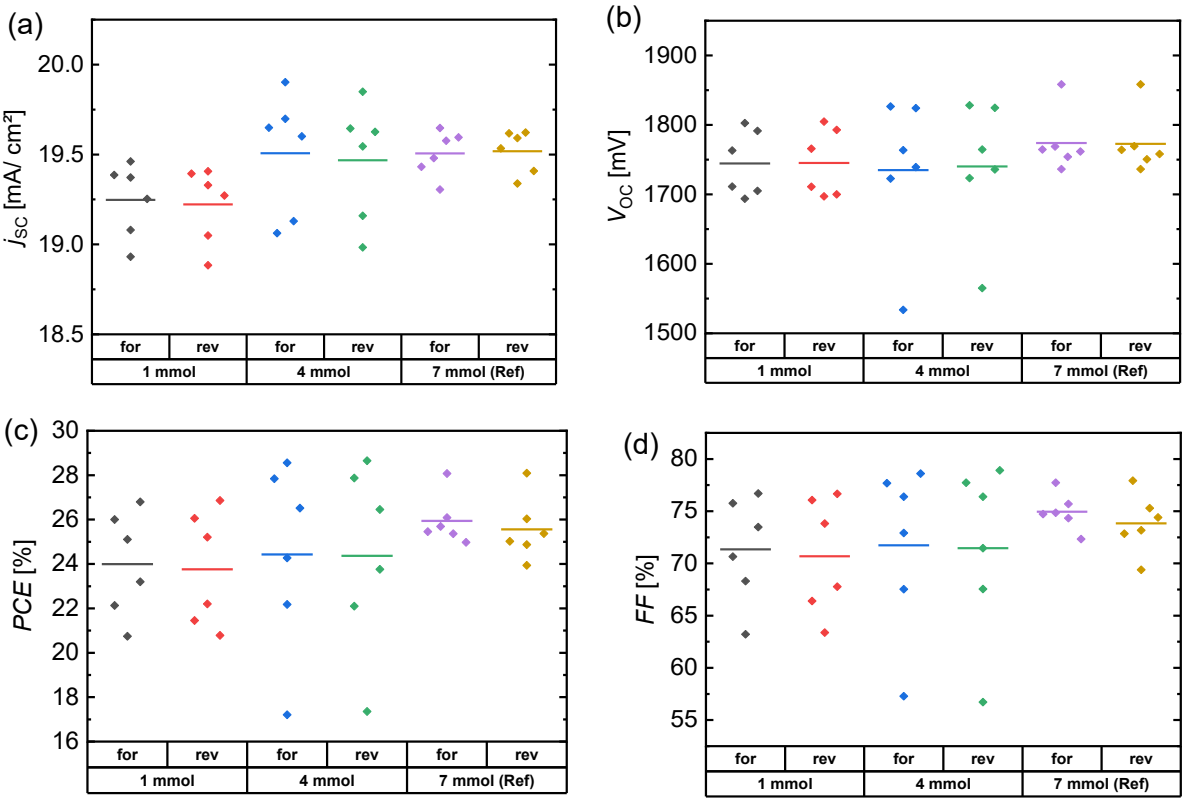

Figure S16. (a, b, c, d) Influence of varying the solution concentration of the 2PACz on the *jV* parameters of perovskite silicon tandems solar cells fabricated in p-i-n configuration. Note that the higher j_{SC} and *PCE* values are due to the use of metallization mask with narrow finger widths, as shown in Figure S23.

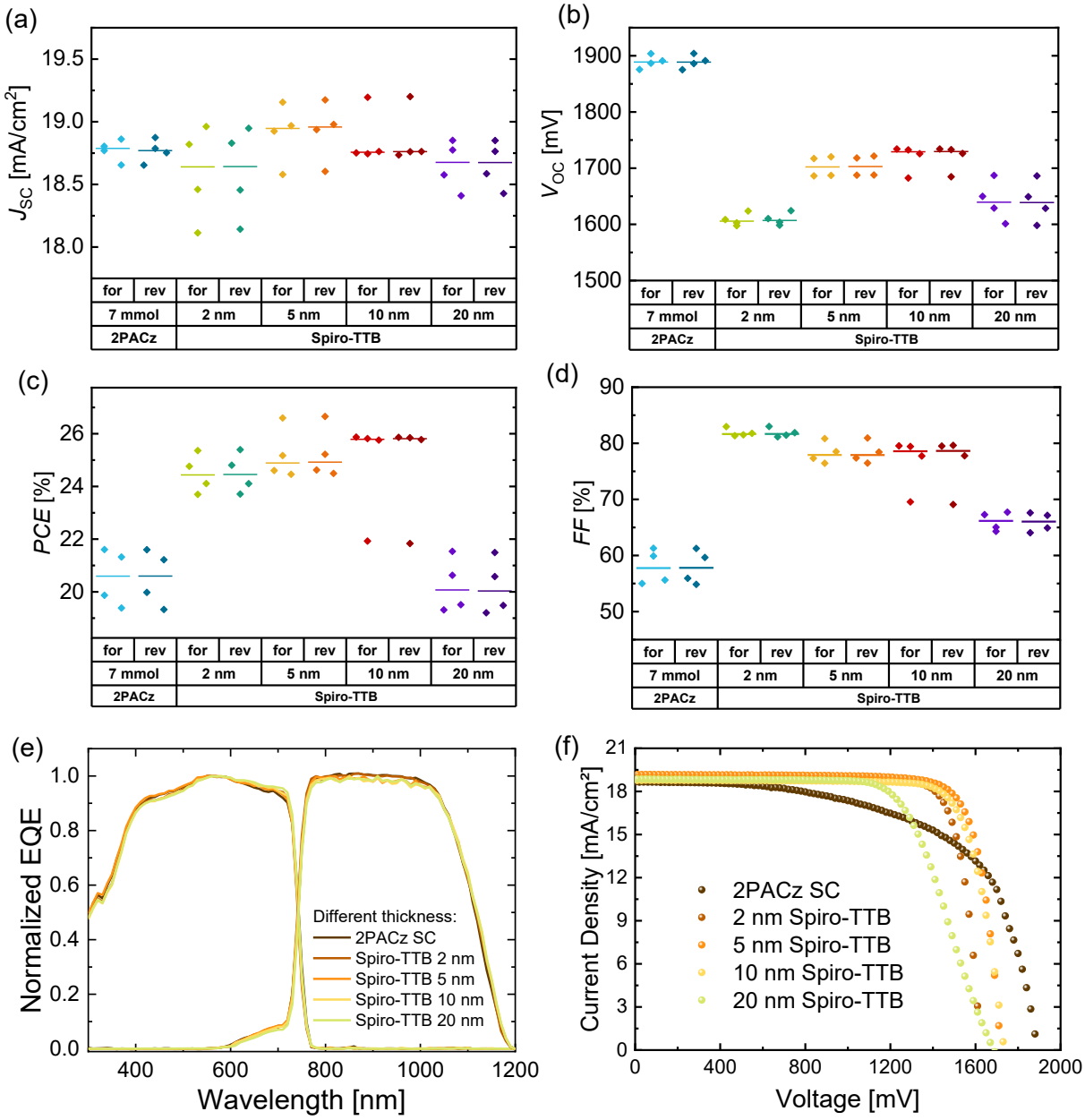

Figure. S17 (a, b, c, d) Influence of varying the thickness of the Spiro-TTB layer on the *jV* parameters of perovskite silicon tandems solar cells fabricated in p-i-n configuration. (e) Normalized *EQE* of tandem solar cells for different thickness of Spiro-TTB. (f) *jV* curves of the best performing cells from each group scanned in reverse direction (V_{OC} to j_{SC}).

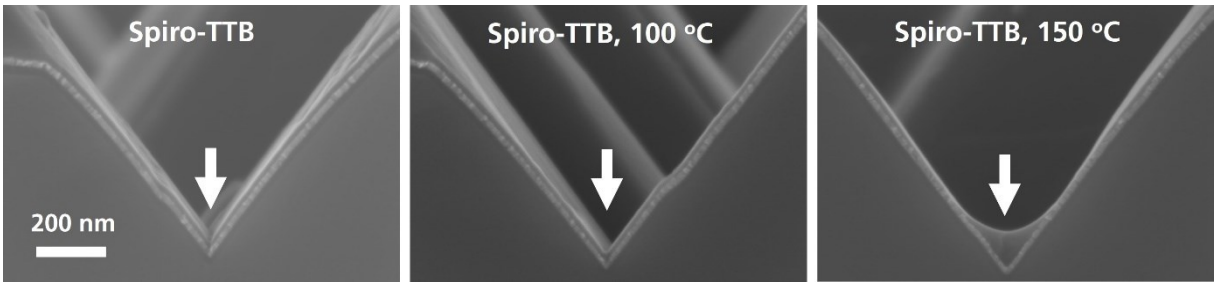

Figure S18. Cross sectional SEM images of thermally evaporated Spiro-TTB (20 nm) on textured substrate (textured Si/ITO/Spiro-TTB stack) as deposited, annealed at 100 °C and 150 °C.

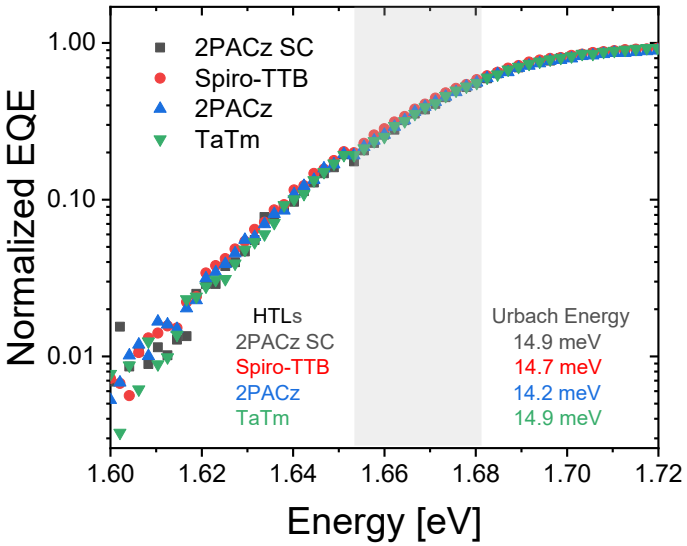

Figure S19. Normalized *EQE* of top perovskite cells with different HTLs, measured with 1 nm step size. The slope in the highlighted region gives an estimate of the Urbach energy.

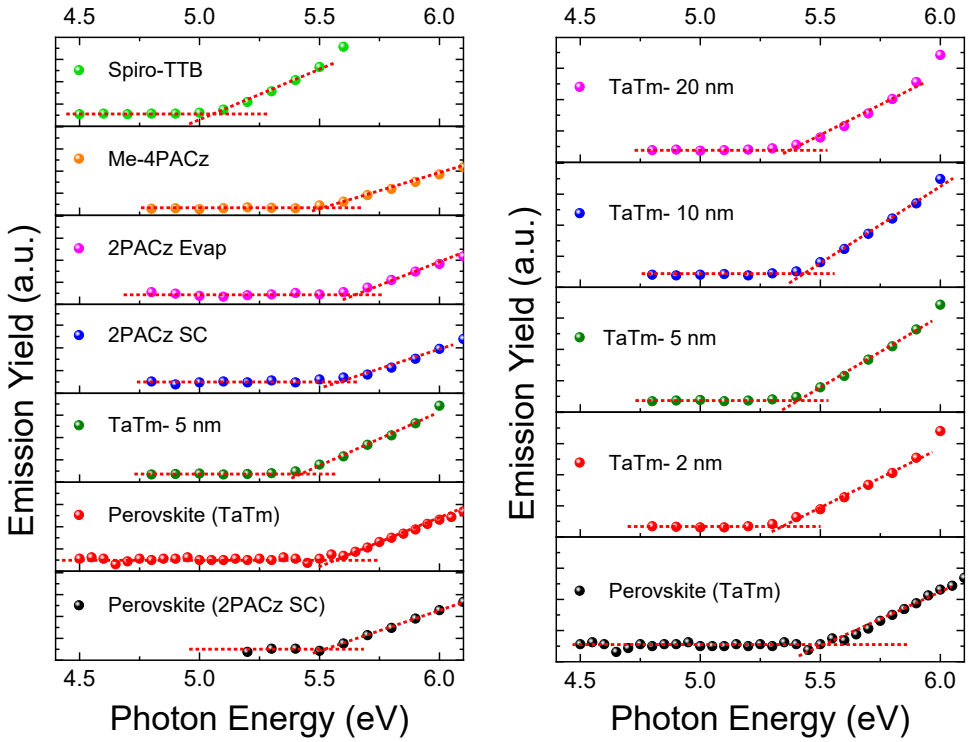

Figure. S20 Photoemission spectroscopy measurements in air (PESA) for different HTLs (2PACz, TaTm, Spiro-TTB and Me-4PACz) deposited on textured substrate with Si/ITO/HTL stack and perovskites deposited on spin coated 2PACz and TaTm- 5 nm with Si/ITO/HTL/perovskite stack illustrating respective valence band maximum (VBM) position.

Table S1. HOMO/VBM of different HTLs and Perovskites (For the estimation of ΔE, energy difference between VBM of perovskite* and HOMO of different HTLs, perovskite processed on 5 nm TaTm was considered as reference)

Layer	VBM (eV)	ΔE* (eV)
2PACz SC	-5.56	0.04
2PACz (4 nm)	-5.51	0.01
TaTm (5 nm)	-5.41	0.14
Spiro-TTB (10 nm)	-5.06	0.5
Me-4PACz (4 nm)	-5.51	0.04
*Perovskite (TaTm)**	-5.55	--
Perovskite (2PACz SC)	-5.51	0.04
TaTm (2 nm)	-5.32	0.23
TaTm (10 nm)	-5.42	0.13
TaTm (20 nm)	-5.36	0.19

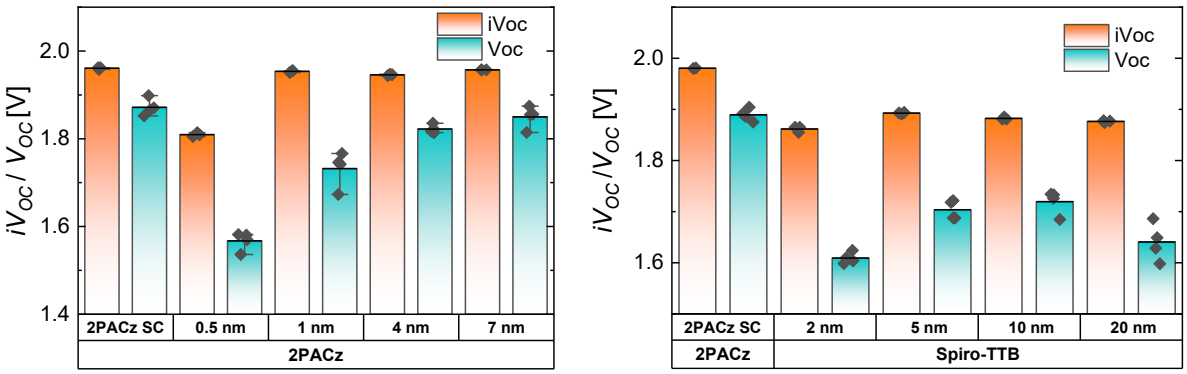

Figure S21. Impact of thickness variation of 2PACz and Spiro-TTB on QFLS/iV_{OC} (perovskite+silicon) extracted from steady-state PL measurements and Voc of the tandem devices extracted from *jV* measurements. For PL measurements textured silicon/ITO/HTL/perovskite stack was used whereas *jV* measurements were performed on final tandem device.

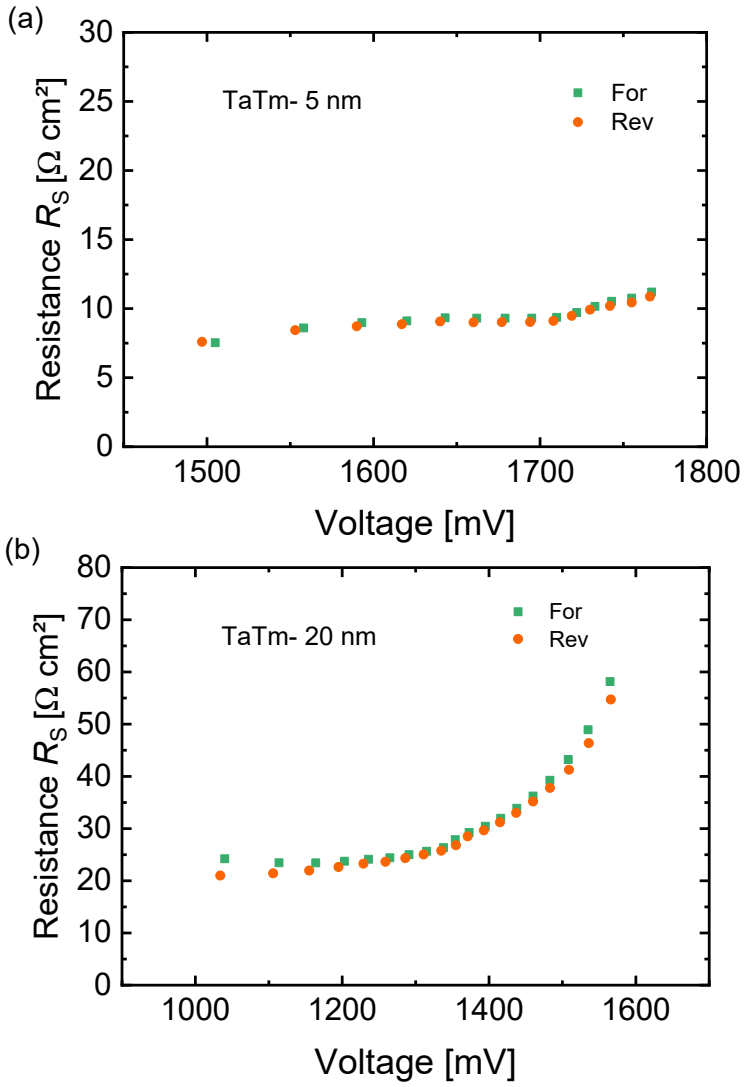

Figure S22. Plot showing variation in effective R_S, extrated from Suns- V_{OC} measurements, over a certain voltage range close to V_{OC} of the tandem device for (a) 5 nm and (b) 20 nm thick TaTm layer.

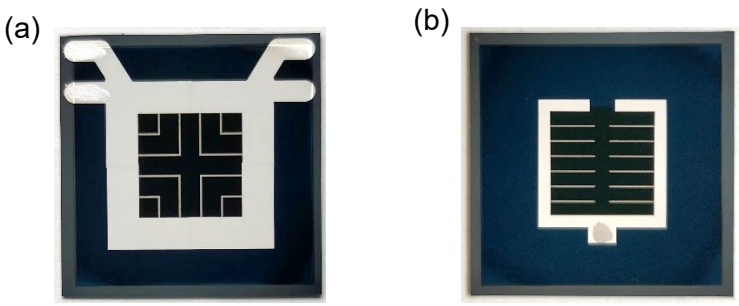

Figure S23. Photograph of perovskite silicon tandem solar cells with two diffrerent metallization designs. (a) Reference metallization mask with L shape fingers and width of ~100 µm, (b) U-shape metallization mask with line shape fingers and width of ~25 µm. The use of design with thinner finger widths (U-shape) facilitates in reducing the shading losses and hence improve the overall j_{SC} of the tandem device. Both reference and U-shape metallization mask have active area of ~1 cm^2.

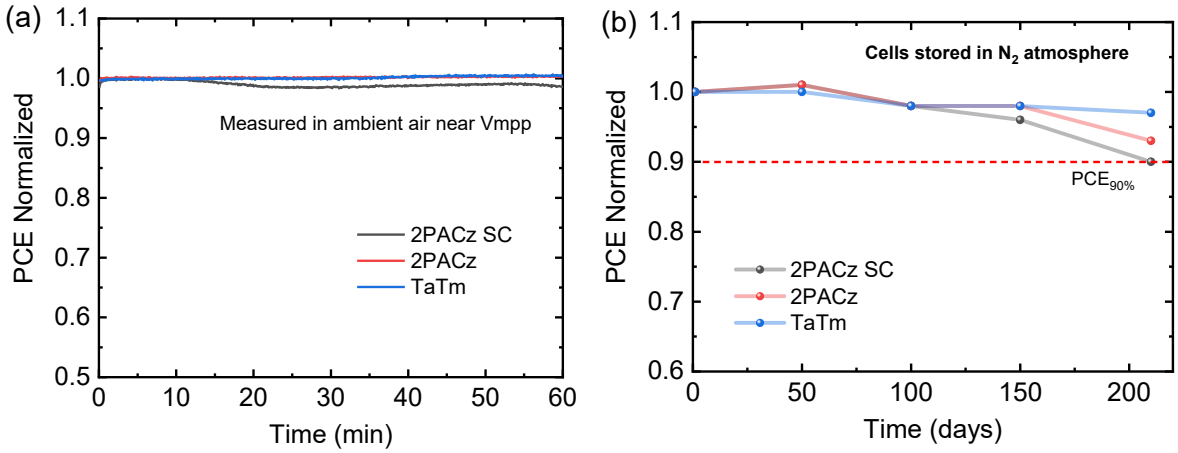

Figure S24. (a) Normalized PCE of the tandem cells with different HTLs under continuous working condition, recorded by applying a voltage close to the maximum power point for 60 mins. (b) Long term stability data of the tandem cells with different HTLs monitored for a period of 210 days. The cells were stored in N_2 atmosphere in dark and taken outside (in ambient atmosphere) for *jV* measurements. The cells with different HTLs retain more than 90% of the PCE over this period.

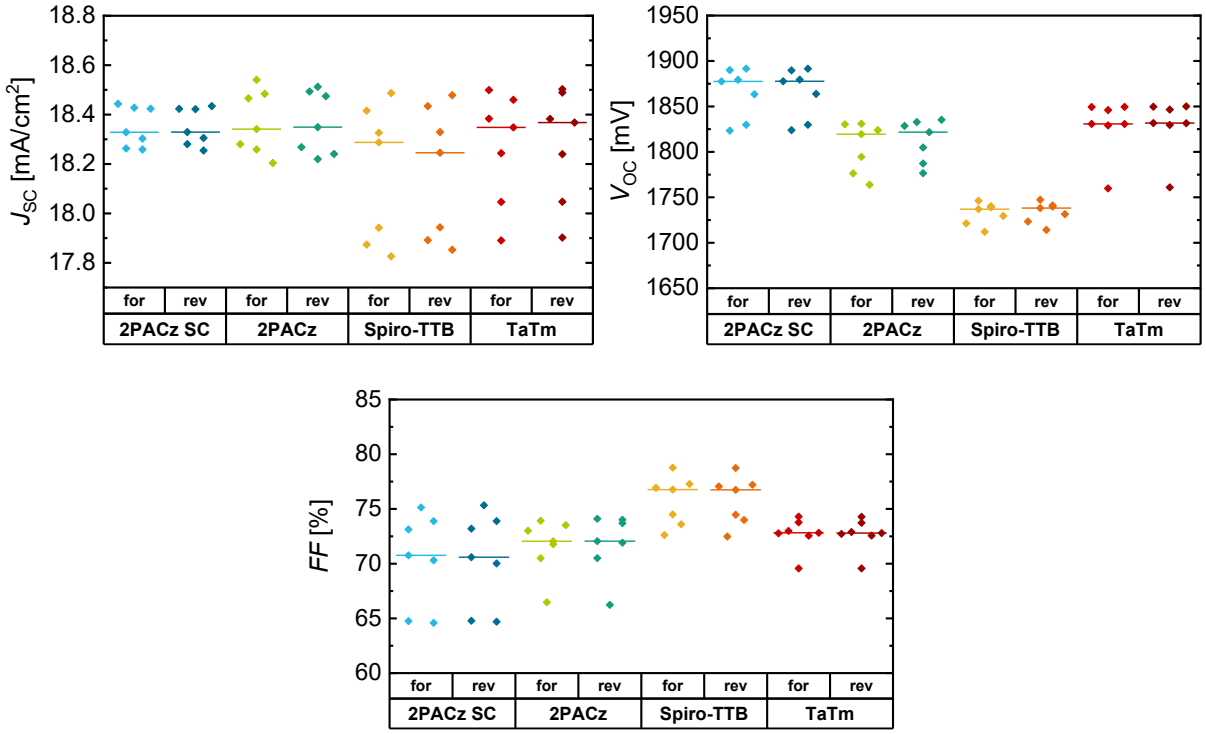

Figure S25. j_{SC}, V_{OC} and *FF* of the tandem devices with different HTLs on 4 cm^2 active area. The median (red line) shows average efficiencies beyond 24% for most of the HTLs used in this study. The j_{SC} are comparable to that of the 1 cm^2 active area tandem devices.

References

1. Meusel M., Adelhelm R., Dimroth F., Bett A., W. Warta W., Spectral mismatch correction and spectrometric characterization of monolithic III-V multi-junction solar cells, Progress in Photovoltaics Res. Appl. 2002; 10: 243-255
2. Heydarian M., Messmer C., Bett A.J., Heydarian M., Chojniak D., Kabaklı Ö.Ş., Tutsch L., Bivour M., Siefer G., Schubert M.C., et al., Maximizing Current Density in Monolithic Perovskite Silicon Tandem Solar Cells. Sol. RRL. 2023; 72200930
3. Bett A.J., Chojniak D., Schachtner M., Reichmuth S.K., Kabaklı Ö.Ş., Schulze P.S.C., Fischer O., Schindler F., Hohl-Ebinger J., Siefer G., et al., Spectrometric Characterization of Monolithic Perovskite/Silicon Tandem Solar Cells., Sol. RRL. 2023; 72200948
4. Fischer O., Bui A.D., Schindler F., Macdonald D., Glunz S.W., Nguyen H.T., Schubert M.C., Versatile Implied Open-Circuit Imaging Method and its Application in Monolithic Tandem Solar Cells., Progress in Photovoltaics. 2023; 1-14.